



## NRC Publications Archive Archives des publications du CNRC

### **Evaluation of astrometry errors due to the optical surface distortions in adaptive optics systems and science instruments**

Ellerbroek, Brent; Herriot, Glen; Suzuki, Ryuji; Schoeck, Matthias

This publication could be one of several versions: author's original, accepted manuscript or the publisher's version. / La version de cette publication peut être l'une des suivantes : la version prépublication de l'auteur, la version acceptée du manuscrit ou la version de l'éditeur.

For the publisher's version, please access the DOI link below. / Pour consulter la version de l'éditeur, utilisez le lien DOI ci-dessous.

#### **Publisher's version / Version de l'éditeur:**

<http://doi.org/10.12839/AO4ELT3.13285>

*Third AO4ELT Conference - Adaptive Optics for Extremely Large Telescopes, 2013-05-26*

#### **NRC Publications Record / Notice d'Archives des publications de CNRC:**

<http://nparc.cisti-icist.nrc-cnrc.gc.ca/eng/view/object/?id=61220a3d-cde1-4e7e-888d-ad4b73a2c7>

<http://nparc.cisti-icist.nrc-cnrc.gc.ca/fra/voir/objet/?id=61220a3d-cde1-4e7e-888d-ad4b73a2c74b>

Access and use of this website and the material on it are subject to the Terms and Conditions set forth at

<http://nparc.cisti-icist.nrc-cnrc.gc.ca/eng/copyright>

READ THESE TERMS AND CONDITIONS CAREFULLY BEFORE USING THIS WEBSITE.

L'accès à ce site Web et l'utilisation de son contenu sont assujettis aux conditions présentées dans le site

<http://nparc.cisti-icist.nrc-cnrc.gc.ca/fra/droits>

LISEZ CES CONDITIONS ATTENTIVEMENT AVANT D'UTILISER CE SITE WEB.

**Questions?** Contact the NRC Publications Archive team at

PublicationsArchive-ArchivesPublications@nrc-cnrc.gc.ca. If you wish to email the authors directly, please see the first page of the publication for their contact information.

**Vous avez des questions?** Nous pouvons vous aider. Pour communiquer directement avec un auteur, consultez la première page de la revue dans laquelle son article a été publié afin de trouver ses coordonnées. Si vous n'arrivez pas à les repérer, communiquez avec nous à PublicationsArchive-ArchivesPublications@nrc-cnrc.gc.ca.





# EVALUATION OF ASTROMETRY ERRORS DUE TO THE OPTICAL SURFACE DISTORTIONS IN ADAPTIVE OPTICS SYSTEMS and SCIENCE INSTRUMENTS

Brent Ellerbroek<sup>1a</sup>, Glen Herriot<sup>2</sup>, Ryuji Suzuki<sup>3</sup>, and Matthias Schoeck<sup>1</sup>

<sup>1</sup> TMT Observatory Corporation, Instrumentation Department, 1111 S. Arroyo Pkwy, Pasadena, CA, 91107 USA

<sup>2</sup> National Research Council Canada, NRC Herzberg Institute of Astrophysics, 5071 West Saanich Road, Victoria, British Columbia, V9E 2E7 Canada

<sup>3</sup> National Astronomical Observatory of Japan, TMT Project Office, Osawa 2-21-1, Mitaka, Tokyo, 181-8588 Japan

**Abstract.** The objectives for high precision astrometry on ELTs will be challenging, with requirements in the range from 10 to 50 micro-arc-seconds for some instruments and science cases. Reducing and correctly calibrating the systematic and quasi-static errors introduced by optical surface distortions will be an important part of meeting these goals. In a recently submitted paper, we described an analytical Fourier domain model for evaluating these effects as the sum of three terms: (i) under-sampling errors, due to measuring the effects of static surface distortions using a finite number of discrete reference sources; (ii) unknown beam wander across the static surface distortions due to line-of-sight jitter or boresighting errors, and (iii) quasi-static errors due to slowly varying surface distortions. In this paper, we apply these methods to evaluating this term in the astrometry error budgets for the TMT Infrared Imaging Spectrograph (IRIS) and the facility AO system, NFIRAOS. The inputs to this exercise include the original top-down allocations for this error term, the IRIS and NFIRAOS optical system designs, the original optical surface specifications as derived earlier on the basis of wavefront error requirements, our assessment of the feasible density and positioning accuracy for an array of calibration sources, and the expected beam wander due to tip/tilt jitter and bore-sighting errors between NFIRAOS and IRIS. The astrometry error initially computed for NFIRAOS was considerably larger than the top-down allocation due to the contributions from the system's double-pane entrance window, which is close to the system's input focal plane. The error can be reduced to fall within the allocation by defining tighter, but still feasible, specifications for these elements. The astrometry errors computed for two different optical design options for IRIS are significantly different, and depend upon the proximity of the first IRIS fold mirror to the intermediate focal plane located between NFIRAOS and IRIS.

## 1 Introduction

A recent paper [1] has developed a set of engineering formulas for estimating the astrometry, or image distortion, errors resulting from optical surface aberrations in science instruments and their associated adaptive optics (AO) systems. The formulas are based upon a simplified Fourier domain model, with the aberrations on each optical surface modeled as statistically stationary “phase screens” located at one or several conjugate ranges from the optical system pupil. Starting with such assumptions, the formulas obtained are consequently somewhat similar to analytical models for the effects of tip/tilt anisoplanatism in AO, and are sufficiently simple to use for

---

<sup>a</sup> brente@caltech.edu

developing error budgets and setting optical surface requirements for science instruments and AO systems.

In this study, we apply these results to estimate the expected impact of static optical surface aberrations on astrometric accuracy for the Thirty Meter Telescope (TMT) first light instrument IRIS [2] and its associated AO system NFIRAOS [3]. The analysis is based upon the current (as of May 2013) optical designs for these systems and the optical surface error specifications previously derived from top-level system requirements on the allowable RMS wavefront error. For both systems, we find that optical surfaces located close to intermediate focal planes can be a significant source of image distortion errors unless (i) their optical surface aberrations are reduced to a few nm RMS, which approaches the requirements of high contrast imaging systems, and/or (ii) the image distortion effects can be accurately calibrated using a dense array of stable reference sources. In the case of NFIRAOS, the wavefront quality requirements for a double-pane entrance window located relatively close to the TMT focal plane are on the order of 3-5 nm RMS in order to achieve image distortion errors (after calibration) at the desired level of  $5 \mu$  arc sec. For one IRIS optical design option, the requirements on wavefront quality for a pair of input fold mirrors are similar, even if a very dense array of reference sources (possibly  $30 \times 30$  or  $60 \times 60$  sources across a 15 arc sec field of view) is utilized for calibration.

The rest of the paper is organized as follows. Section 2 is a brief summary of the main elements of the Fourier domain model used for computing the image distortion errors due to optical surface aberrations. Section 3 presents the optical designs for the NFIRAOS and IRIS systems, at least as envisaged in May 2013 at the time of the AO4ELT3 conference. Section 4 presents results obtained for the image distortion calibration errors due to static optical surface aberrations. Section 5 is a brief conclusion with some recommendations for future work.

## 2 Outline of the Fourier domain model

As stated previously, we have used first order, geometric optics to model the focal plane image distortions due to optical surface aberrations. These aberrations on each optical element are assumed to be random with shift-invariant statistics, or in other words defined in terms of a power spectral density (PSD) in the spatial frequency domain. Each of these optical surface aberrations is treated as a “phase screen” conjugate to some range from the telescope entrance pupil, and the overall wavefront error due to the combined effects of all the optical surfaces is just the sum of the contributions at each surface. Lastly, the resulting image distortion at each field point is computed as the RMS best-fit tilt to this overall wavefront profile. Using the above model, the RMS image distortion due to optical surface aberration in a single observation of the science field can be developed using Fourier domain techniques.<sup>1</sup>

Fig. 1 illustrates how the image distortion errors in a single observation determine either absolute or differential astrometry errors after initial calibration and post-processing of one or several images. The effects of static optical surface aberrations may be calibrated using either a grid of artificial reference sources or on-sky observations of dense star fields, but these methods cannot account for the image distortions beyond the Nyquist frequency of the reference source grid. Additional sources of image distortion include quasi-static wavefront errors which occur between the calibration measurements and the science exposures, or boresight (alignment) errors which cause beams to translate across the optical surfaces. These time-varying errors may

<sup>1</sup> Other simplifying assumptions used to develop the model include (i) a circular, unobscured telescope aperture, (ii) a circular field of view, and (iii) circularly symmetric PSDs for the optical surface errors.

be calibrated using field stars with accurately known coordinates within the science field. For differential astrometry the effect of truly static aberrations will cancel out, but the effects of time-varying wavefront errors in multiple observations must still be accounted for.

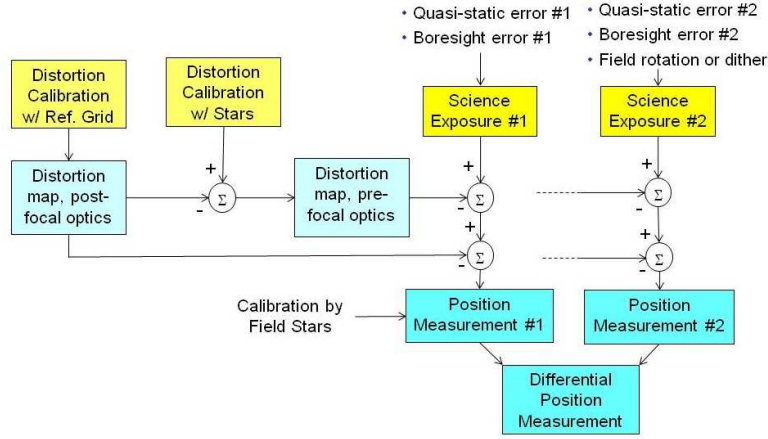


**Fig. 1.** Observing sequence model for determining image distortion from optical surface errors

For completeness, the principal formulas derived in [1] to evaluate these image distortion errors are as follows:

- Quasi-static optical surface aberrations:

$$\sigma_i^2 = \left(\frac{\lambda}{D}\right)^2 \left(\frac{2}{\pi}\right)^2 \iint d\mathbf{v} \Phi_i(\mathbf{v}) \left| \frac{4J_2(\pi D\mathbf{v})}{\pi D\mathbf{v}} \right|^2 \left[ 1 - \sum_{m=0}^M \left| \frac{(m+1)J_{m+1}(2\pi\rho h_i \mathbf{v})}{\pi\rho h_i \mathbf{v}} \right|^2 \right]. \quad (1)$$

- Deterministic beam translation across surfaces:

$$\sigma_i^2 = \left(\frac{\lambda}{D}\right)^2 \left(\frac{2}{\pi}\right)^2 \iint d\mathbf{v} \Phi_i(\mathbf{v}) \left| \frac{4J_2(\pi D\mathbf{v})}{\pi D\mathbf{v}} \right|^2 [2 - 2J_0(2\pi h_i \delta \mathbf{v})] \times \left[ 1 - \sum_{m=0}^M \left| \frac{(m+1)J_{m+1}(2\pi\rho h_i \mathbf{v})}{\pi\rho h_i \mathbf{v}} \right|^2 \right]. \quad (2)$$

- Imperfect calibration of static surface aberrations:

$$\sigma_i^2 = 2 \left(\frac{\lambda}{D}\right)^2 \left(\frac{2}{\pi}\right)^2 \iint_{\|\mathbf{v}\|_\infty > (2h_i d)^{-1}} d\mathbf{v} \Phi_i(\mathbf{v}) \left| \frac{4J_2(\pi D\mathbf{v})}{\pi D\mathbf{v}} \right|^2. \quad (3)$$

Here  $\sigma_i^2$  is the one-axis RMS image distortion due to optical surface errors on surface number  $i$ ,  $\lambda$  is the observation wavelength, and  $D$  is the telescope aperture diameter.  $\Phi_i$  is the PSD describing the wavefront (not surface) aberration on surface number  $i$ , and  $\mathbf{v}$  is a two-dimensional spatial frequency variable. In Eq. (3), the conjugate range of surface number  $i$  is denoted  $h_i$ , and  $d$  is the angular spacing of the grid of artificial calibration sources. In Eq. (2),  $\delta$  is the magnitude of the angular alignment error introducing the beam translation. In Eq.'s (1) and (2),  $M$  is the order of the image distortion modes calibrated using field stars ( $M = 0$  for overall tip/tilt,  $M = 1$  for plate scale, etc.), and  $\rho$  is the radius of the circular field-of-view.

### 3 NFIRAOS and IRIS optical systems

Fig. 2 illustrates the optical design of the NFIRAOS science path as of May, 2013, together with the 3-mirror TMT. The science path optics include a double-pane entrance window, a total of 4 off-axis parabolas, two deformable mirrors (DMs) optically conjugate to ranges of 0.0 and 11.2 km from the TMT primary mirror, M1, and the “science beamsplitter” which reflects visible light ( $\lambda \leq 0.8 \mu\text{m}$ ) to the NFIRAOS wavefront sensors. The optical surface nearest to focus is evidently the double-pane entrance window.

For this analysis, we originally assumed the same wavefront specifications derived for each surface from the NFIRAOS on- and off-axis wavefront quality requirements. These specifications are consistently close to 25 nm RMS for each optical element (including both of the entrance windows), with a 2-dimensional spatial PSD proportional to  $\kappa^{-p}$  where  $p = 2.5$ .<sup>2</sup> The results in Sec. 4 below demonstrate that these requirements are too loose for the entrance windows, which are now specified (after vendor discussions) to have a tighter requirement of only 3 nm RMS with the same power law.

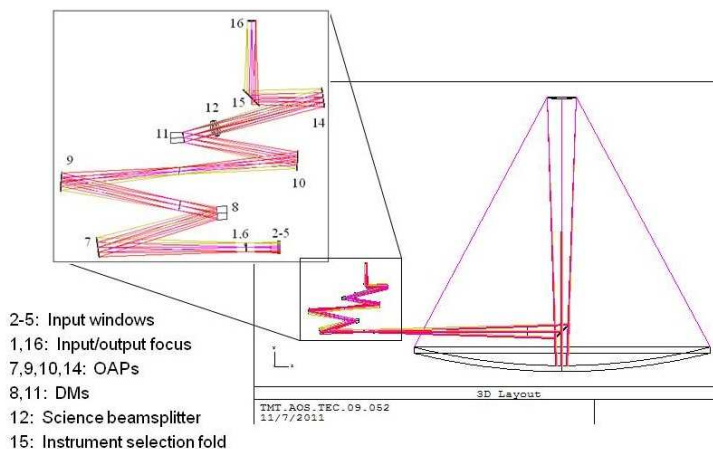


**Fig. 2.** NFIRAOS and TMT optical designs (as of May, 2013)

Fig. 3 illustrates one of two options currently under consideration for the IRIS imaging channel. Both options include essentially the same refractive collimating optics, a collimated space for filters and a cold stop, and a reflective three mirror anastigmatic (TMA) camera. The illustrated design option also includes a pair of fold mirrors immediately following the input focal plane. This configuration permits the IRIS imaging channel to be duplicated within the IRIS dewar, thereby doubling the total imager field of view. This improvement must be weighted against the placement of the fold mirrors close to focus, which will complicate the calibration of the image distortion due to these surfaces.<sup>3</sup>

For this analysis, we have assumed a  $\lambda/20$  peak-to-valley surface aberration on each optical element in IRIS, corresponding to an RMS wavefront error of  $xxx$  nm. Higher quality optics are consequently one option to reduce the image distortion errors estimated in Sec. 4 below.

<sup>2</sup> The RMS wavefront error is specified within the entire clear aperture of the optic, with tip, tilt and focus removed.

<sup>3</sup> It should be noted that the optical design for the a single imaging channel also includes two fold mirrors. They are located following the entrance window to the IRIS dewar, at a somewhat greater distance from the input focal plane.

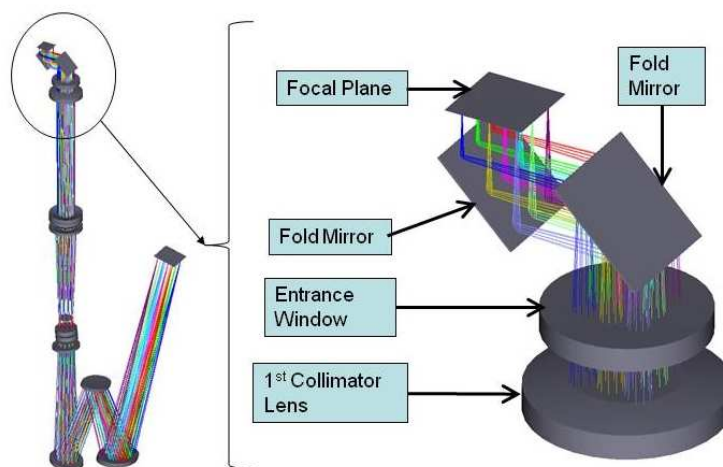


Fig. 3. IRIS imager optical design including fold mirrors for implementing dual imaging channels

## 4 Image distortion calibration errors due to static optical surface aberrations

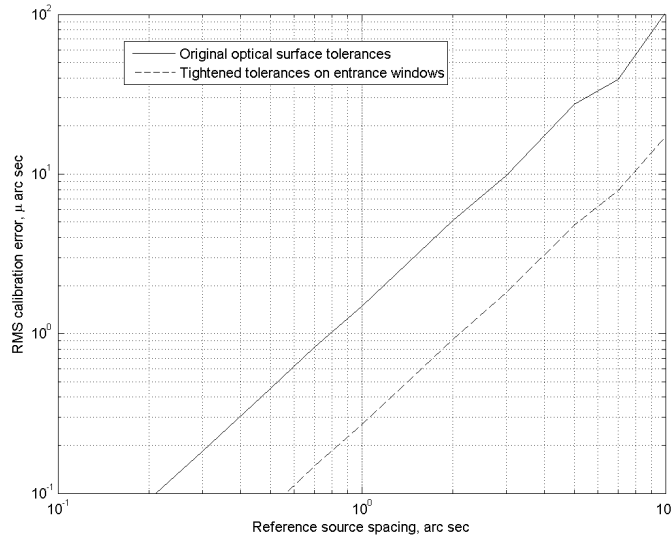
### 4.1 NFIRAOS

Fig. 4 illustrates the image distortion calibration errors predicted due to optical surface aberrations in NFIRAOS as a function of the density assumed for the reference source grid. Results are presented for both the original optical surface specifications (solid line), and tightened specifications for the double-pane entrance window (dashed). It can be seen that tightening these tolerance has reduced the image distortion error by roughly a factor of four for a given reference source spacing, or alternatively has relaxed the source spacing required for a given image distortion error by roughly a factor of 2.5. For example, the reference source spacing required for an image distortion error of  $5 \mu$  arc sec RMS is about 2 (or 5) arc sec for the original (or revised) tolerances on the dual pane input window.

Fig. 5 plots the cumulative RMS image distortion calibration error as a function of the number of NFIRAOS optical surfaces considered. The surfaces errors are summed from the least-to-most sensitive surface, and a reference source spacing of  $5 \mu$  arc sec on the sky is assumed. The large majority of the image distortion error calibration was originally contributed by the two most sensitive optical elements, which are the entrance windows. Tightening the wavefront quality specifications for these two optics from 25 to 3 nm RMS reduces the end-to-end image distortion error from about 30 to  $5 \mu$  arc sec for this reference spacing.

### 4.2 IRIS

Fig. 6 illustrates the RMS image distortion calibration error due the IRIS optics as a function of reference source spacing. The calibration errors for the dual-channel design are considerably larger on account of the location of the fold mirrors, and the reference source spacing must be reduced by approximately a factor of four to match the image distortion error for the single-channel design. Even with the single-channel design, a source spacing of 0.8–1.0 arc sec is required to achieve a distortion calibration error in the range of  $5\text{--}8 \mu$  arc sec.



**Fig. 4.** Image distortion calibration error due to NFIRAOS optical surface aberrations vs. reference source spacing

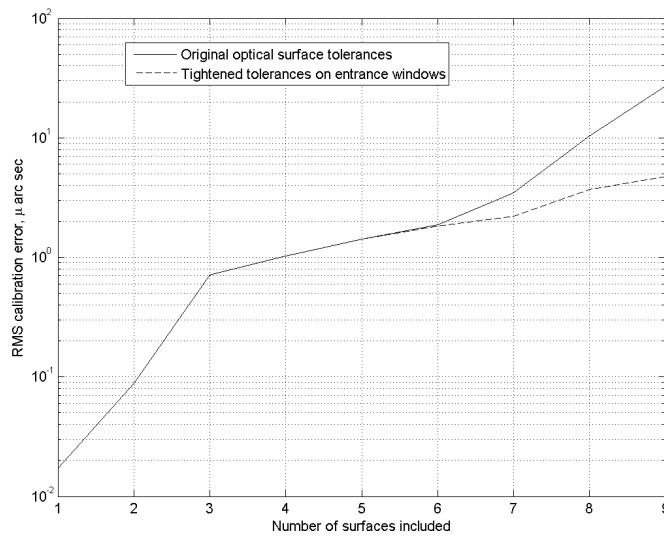


**Fig. 5.** Cumulative contribution of image distortion calibration errors by optical surfaces in NFIRAOS for a 5 arc sec reference source spacing

Fig. 7 plots the cumulative image distortion calibration error for a reference source spacing of 1 arc sec as a function of the number of surfaces included, again beginning with the surfaces with the smallest contributions. The significance of the errors contributed by the pair of fold mirrors in the dual imager design is apparent.

## 5 Conclusion

We have applied a Fourier domain model for evaluating the image distortion calibration errors due to static optical surface aberrations to the particular case of the TMT science instrument

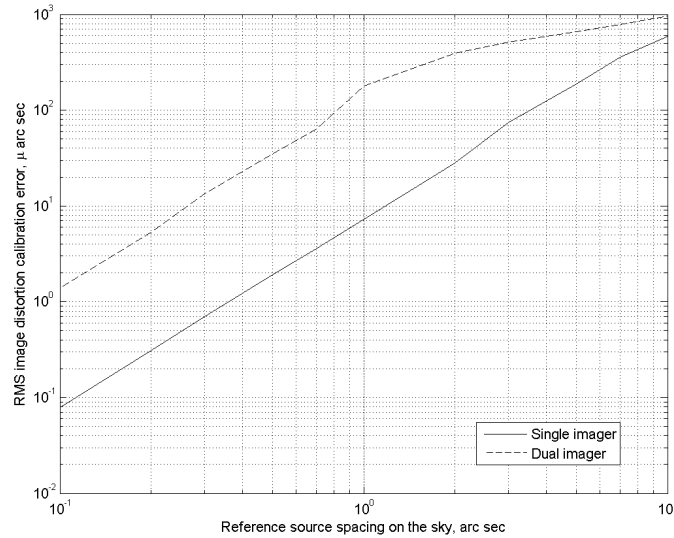


**Fig. 6.** Image distortion calibration error due to IRIS optical surface aberrations vs. reference source spacing

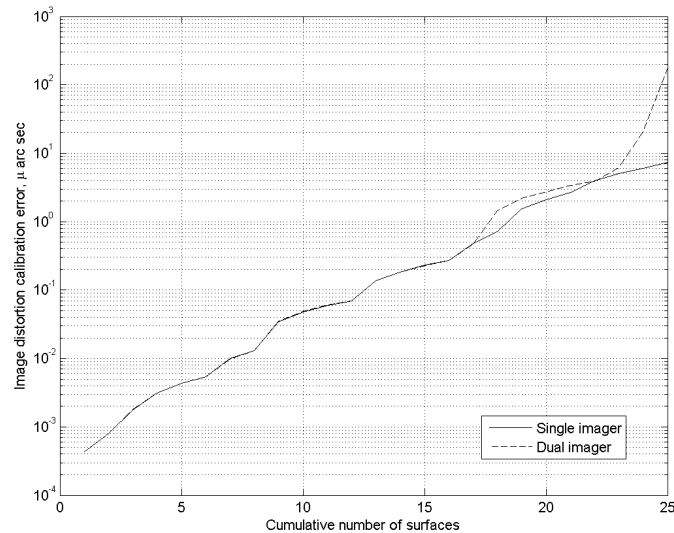


**Fig. 7.** Cumulative contribution of image distortion calibration errors by optical surfaces in IRIS for a 1 arc sec reference source spacing

IRIS and facility AO system NFIRAOS. Similar calculations (not reported here due to space limitations) have investigated the differential image distortions resulting from quasi-static surface aberrations on deformable mirrors [4] and beam wander across optics due to alignment errors. These results begin to quantify the contributions of optical surface aberrations to the overall astrometry error budget [5]. In particular, the results in this paper highlight the particular significance of aberrations on optical surfaces located close to intermediate focal planes, in much the same way as atmospheric turbulence at high altitude has a disproportionate impact upon the isoplanatic angle of an adaptive optics system. A high density of reference sources is needed to calibrate the effects of these surfaces. Of course, the required number of reference sources

can be reduced by improving the surface quality of these optics. In some cases, the resulting requirements may be similar to the specifications found in high contrast imaging systems.

The results presented here are based upon a first-order Fourier model, and it is easy to identify a variety of possible refinements to the theory used and the parameters which have been assumed. Some of these include

- The optical surface PSDs for high precision optical surfaces with RMS wavefront errors of a few nm or less;
- How to characterize the impact of edge rolloff, mount print-through, and other surface errors which are not spatially stationary and consequently not accurately modeled by a spatial PSD;
- More sophisticated models for the image distortion calibration error (e.g., something beyond a simple spatial cutoff frequency), and how it depends upon the characteristics of the reference source grid. It may not be possible to specify or even measure the absolute positions of the reference sources to the level of a few micro arcseconds (on the sky), in which case calibration algorithms must be based upon differential position measurements. A model for on-sky calibration techniques using (for example) open star clusters is also required.

These topics will be investigated further as the development of observing methods, and the derived design requirements, for high precision astrometry with IRIS and NFIRAOS proceeds.

## Acknowledgments

The TMT Project gratefully acknowledges the support of the TMT collaborating institutions. They are the Association of Canadian Universities for Research in Astronomy (ACURA), the California Institute of Technology, the University of California, the National Astronomical Observatory of Japan, the National Astronomical Observatories of China and their consortium partners, and the Department of Science and Technology of India and their supported institutes. This work was supported as well by the Gordon and Betty Moore Foundation, the Canada Foundation for Innovation, the Ontario Ministry of Research and Innovation, the National Research Council of Canada, the Natural Sciences and Engineering Research Council of Canada, the British Columbia Knowledge Development Fund, the Association of Universities for Research in Astronomy (AURA) and the U.S. National Science Foundation.

## References

1. Ellerbroek, B., *A&A* **552**, (2013) A41
2. Larkin, J. et al., The Infrared Imaging Spectrograph (IRIS) for TMT: Instrument Overview, published in SPIE Proceedings Volume 7735: Ground-based and Airborne Instrumentation for Astronomy III, 2010
3. Herriot, G. et al., TMT NFIRAOS: adaptive optics system for the Thirty Meter Telescope, published in SPIE Proceedings Volume 8447: Adaptive Optics Systems III, 2012
4. Ellerbroek, B. et al., TMT adaptive optics program status report, published in SPIE Proceedings Volume 8447: Adaptive Optics Systems III, 2012
5. Schoeck, M., Developing Performance Estimates for High Precision Astrometry with TMT, this volume